NASA Technical Memorandum 105297

Effects of Anisotropic Conduction and Heat Pipe Interaction on Minimum Mass Space Radiators

Karl W. Baker
Lewis Research Center
Cleveland, Ohio

and

Kurt O. Lund
University of California, San Diego
San Diego, California

Prepared for the
International Solar Energy Conference
sponsored by the American Society of Mechanical Engineers
Maui, Hawaii, April 4–8, 1992

NASA

f fin

ℓ heat pipe wick/liquid

p pipe

r radiation

s sink

v vapor

INTRODUCTION

Because of its importance for space power and thermal management, heat rejection in space radiators has received considerable attention over the years. Basic results of heat rejection studies have been reported in texts on radiation (Sparrow and Cess, 1978; Edwards, 1981). Minimum mass designs were addressed in 1960 (Bartas and Sellers, 1960); more recently, comparisons have been made between pumped-loop and heat-pipe radiators (Furukawa, 1981), with finned heat-pipes being the choice today.

Despite the extensive previous work, much of which is summarized by Furukawa (1981), there is still interest in the problem as new materials are introduced (McDanels et al., 1991) and as larger power plants are considered for space applications. In particular, new anisotropic composites, where the transverse thermal conductivity may be an order of magnitude less than along the fiber axis (Rhee et al., 1991; Rovang et al., 1991; Materials and Science Corporation, 1986), have raised questions about anisotropic conduction effects in the radiation fins. Furthermore, despite the extensive use of heat-pipe radiator designs, the effective heat-pipe/radiator-fin interaction has not been addressed, with previous analyses using the standard specified root-temperature boundary condition.

The present paper seeks to address these shortcomings, as well as to investigate several minimum-mass heat-pipe radiator designs. Two-dimensional, anisotropic heat conduction equations are formulated for plane fins with radiative conditions on the surfaces. These are reduced to axial integration using integral techniques (Kakac and Yener, 1985), with anisotropic effects contained in a surface radiation Biot number. Effective fin/heat-pipe boundary conditions, and a shape factor are introduced following previous examples (Lund, 1986, 1989). The axial integration was carried out numerically, with approximately 100 steps along the length of the fin, and fin performance curves were derived. Typical designs were analyzed for minimum mass using the performance curves, and an optimum fin length, for various fin efficiencies and for heat-pipe vapor temperatures of 400 and 800 K. It was found that an efficiency of 0.5 yields the minimum mass, which agreed with previous results (Sparrow and Cess, 1978; Bartas and Sellers, 1960); however, it is a very flat minimum, and other efficiency values can be used at the designer's option without incurring significant penalty.

Even at the higher temperature, the Biot number was found to be a very small number, such that anisotropic effects are negligible for the cases considered. Overall, conduction affects the minimum-mass designs as a weak function, as compared to the material density, and carbon/carbon composites had the lowest mass of the designs considered. The effect of the interface shape factor was also evaluated.

Minimum-mass radiator designs have particular importance for overall space power system design, as was indicated for solar dynamic power (Lund, 1990). However, radiators in actual systems operate under many constraints not considered here; in this sense, the present analysis may be considered as an unconstrained optimization problem. Although many diverse effects are not considered, the results nevertheless provide a guide to limits of performance of plane fin/heat-pipe radiators using recently developed materials.

THERMAL ANALYSIS

The thermal analysis of the space radiator considered here may be divided into the following parts: (a) radiation-enclosure analysis of the exterior to the radiator fin, or panel; (b) conduction analysis internal to the fin; (c) analysis of the heat-pipe condenser adjoining the panels; and (d) the interaction between these effects. Here the objective is to separate each effect, as much as possible, by the introduction of fin efficiency, effective surface conductances, and shape factors. This simplifies the model equations, as well as generalizes the results to a wider class of designs, as shown previously (Lund, 1986, 1989).

Exterior Radiation Model

We consider an element of radiator fin, as shown in Fig. 1, where the net heat rates (per unit width) leaving the element from

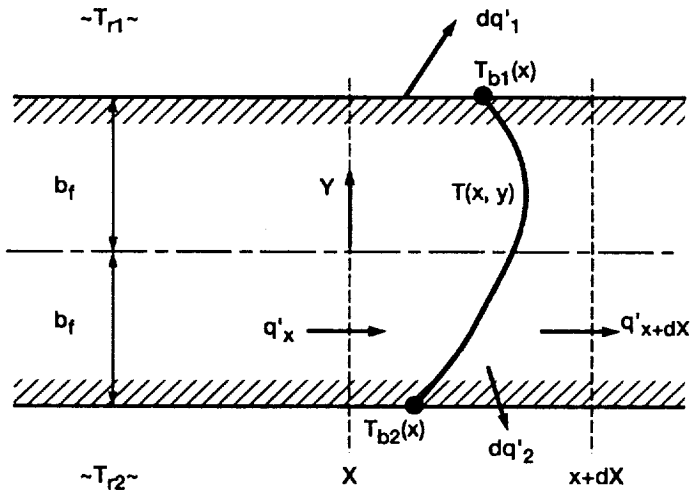

Figure 1.—Control volume for integral analysis of fin.

surfaces 1 and 2 are dq_1', and dq_2', and where the corresponding surface temperatures at the location X are T_{b1} and T_{b2}. Assuming these surfaces to be gray (diffuse with constant emissivities), and exchanging radiant energy with surrounding gray surfaces (j at temperature T_{sj}), the net heat rate from one side of the element (say, side 1), may be stated as

$$dq_1 = \sum_J \mathcal{F}_{1j}\sigma\left(T_{b1}^4 - T_{sj}^4\right)dA \tag{1}$$

where $\mathcal{F}$ is the usual gray-body view factor, or transfer function (e.g., Siegel and Howell, 1981; Edwards, 1981), which satisfies the summation

$$\sum_j \mathcal{F}_{1j} = \epsilon_1 \tag{2}$$

Combining Eqs. (1) and (2) results in the exterior radiation model

$$dq_1' = \epsilon_1\sigma\left(T_{b1}^4 - T_{r1}^4\right)dA \tag{3}$$

where the surface-1 effective radiation temperature of the surroundings is

$$T_{r1}^4 = \frac{1}{\epsilon_1}\sum_j \mathcal{F}_{1j}T_{sj}^4 \tag{4}$$

with similar results for surface 2. Thus, the external radiation problem reduces to determination of the T_r's (which may have some X-dependence through the transfer functions).

In the space environment, however, the effect of the radiation temperature is small. Even if the heat-pipe condenser temperature is as low as 600 K and the surrounding radiation temperature is as high as 300 K, this is a ratio of only 0.5 for which there is negligible effect on the overall rate of heat transfer, or fin efficiency (Sparrow and Cess, 1978; Edwards, 1981). Therefore, for the remainder of the present analysis, T_r will be neglected, which still accounts for most space radiator problems of interest. For ratios greater than 0.5, corrections to the results of the present work can be made with reference to the efficiency curves of Sparrow and Cess (1978). The effect of neglecting T_r is that the fin conduction problem becomes symmetric, regardless of asymmetries in the radiation environs.

Conduction Fin Model

With reference to Fig. 1, an energy balance on the control volume yields

$$q'_X = dq'_1 + q'_{X+dX}$$

or, with Eq. (3),

$$-\frac{dq'_X}{dX} = \varepsilon\sigma T_b^4 \tag{5}$$

where the rate of heat conducted is the integral of the flux over the half cross section. With the axial heat flux related to the axial temperature gradient by the axial conductivity k_x, Eqs. (5) and (6) combine

$$q'_x = \int_0^{b_f} q''_x \, dY \tag{6}$$

as

$$k_x \frac{d^2}{dX^2} \int_0^{b_f} T \, dY = \varepsilon\sigma T^4|_{Y=b_f} \tag{7}$$

On the other hand, the surface heat flux depends on the transverse conductivity k_y, such that the temperature in Eq. (7) must satisfy

$$-k_y \left.\frac{\partial T}{\partial y}\right|_{Y=b_f} = \varepsilon\sigma T^4|_{Y=b_f} \tag{8}$$

and the symmetry condition

$$\left.\frac{\partial T}{\partial Y}\right|_{Y=0} = 0 \tag{9}$$

Based on the assumption that there is negligible heat loss from the tip of the fin, the axial boundary conditions are the insulated tip condition

$$\left.\frac{\partial T}{\partial X}\right|_{X=0} = 0 \tag{10}$$

and an equivalent convection-type condition at the heat-pipe interface

$$k_x \left.\frac{\partial T}{\partial X}\right|_{X=L} = h_e\left(T_e - T|_{X=L}\right) \tag{11}$$

where h_e and T_e are effective parameters (to be determined) associated with particular heat-pipe designs.

Now, introducing the scaled coordinates and temperature $x = X/L$, $y = Y/b$, $\theta = T/T_e$, Eqs. (7) and (8) may be stated as

$$\frac{d^2\bar{\theta}}{dx^2} = N\theta_s^4 \tag{12}$$

$$\left.\frac{\partial\theta}{\partial y}\right|_{y=1} + \beta\theta^4|_{y=1} = 0 \tag{13}$$

where the average and surface temperatures are

$$\bar{\theta} = \int_0^1 \theta \, dy \tag{14}$$

and

$$\theta_s = \theta|_{y=1} \tag{15}$$

and where the radiation/conductance and Biot numbers are

$$N = \varepsilon\sigma T_e^3 L^2/b_f k_x \tag{16}$$

and

$$\beta = \varepsilon\sigma T_e^3 b_f/k_y \tag{17}$$

The effects of transverse and anisotropic conduction are contained primarily in the surface Biot number parameter. These effects have more significance and the parameter becomes larger at higher temperatures and larger fin thicknesses.

A temperature profile which satisfies the centerline symmetry condition and Eq. (15) is given by

$$\theta(x,y) = \theta_c(x) - [\theta_c(x) - \theta_s(x)]y^2 \tag{18}$$

where θ_c is the centerline temperature. Substitition of Eq. (18) into Eq. (13) yields

$$\theta_c = \theta_s + \frac{1}{2}\beta\theta_s^4 \tag{19}$$

and substitution of Eqs. (18) and (19) into Eq. (14) yields the average temperature

$$\bar{\theta} = \theta_s + \frac{1}{3}\beta\theta_s^4 \tag{20}$$

Differentiating Eq. (20) twice and substituting into Eq. (12) then yields the final equation for the surface temperature

$$\left(1 + \frac{4}{3}\beta\theta_s^3\right)\frac{d^2\theta_s}{dx^2} + 4\beta\left(\theta_s\frac{d\theta_s}{dx}\right)^2 - N\theta_s^4 = 0 \tag{21}$$

It is seen that $\bar{\theta}$ is always higher than θ_s by some amount, but that for vanishingly small surface Biot numbers, $\bar{\theta} = \theta_s$, and Eq. (12) reduces to the conventional radiation fin equation. With the integral approximation, Eqs. (7) or (12), the boundary condition (Eq. (11)) cannot be satisfied for all y.

Here we take it to hold in the mean

$$\frac{1}{\gamma}\left.\frac{d\bar{\theta}}{dx}\right|_{x=1} + \bar{\theta}\,|_{x=1} = 1 \tag{22}$$

where the effective end-condition number is

$$\gamma = h_e L/k_x \tag{23}$$

Results of Thermal Model

An example of the numerical integration of Eq. (21), with Eqs. (20) and (22), is shown in Figure 2. The end-condition parameter γ (the heat-pipe interface condition) has considerable effect on the solution; the limit $\gamma \to \infty$ corresponds to the usual, specified root-temperature condition. The difference in surface and average temperatures is also noted for a surface Biot number of 0.2, which accounts for anisotropic conduction effects.

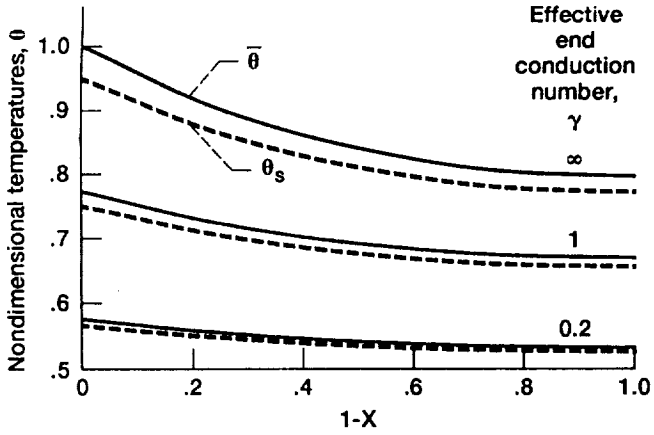

Figure 2.—Typical average and surface temperature distributions in radiator fin for N = 1 and β = 0.2.

Of particular interest is the overall rate of heat transfer through the fin,

$$q_f = \int_0^L q' \, dX = L \, \epsilon\sigma \int_0^1 T_s^4 \, dx$$

or

$$q_f = \eta_f \, L \, \epsilon\sigma T_e^4 \tag{24}$$

where the fin efficiency is give by

$$\eta_f(N,\gamma,\beta) = \int_0^1 \theta_s^4 \, dx \tag{25}$$

This function is shown in Fig. 3. For $\beta = 0.2$, which here accounts for anisotropic conduction, there can be a dramatic effect on efficiency for small N.

From a design and optimization point of view, the radiation/conductance number N is really an unknown since it includes the (as yet) undetermined length or thickness of the fin. Therefore, it is advantageous to invert Eq. (25) and express N as the function $N = N(\gamma,\eta_f,\beta)$. This was accomplished numerically in a double iteration scheme using the simplex algorithm, with results as shown in Fig. 4.

Essentially, for a given fin length and efficiency (and Biot number), N is the inverse fin thickness, (seen the definition, Eq. (16)):

$$b_f = \epsilon\sigma T_e^3 L^2 / k_x N(h_e L/k_x, \; \eta_f, \beta) \tag{26}$$

Thus, for a selected fin efficiency and Biot number, a curve-fit of Figure 4 may be used to determine b_f directly (and iteratively if β is not known, but is to be calculated).

Heat-Pipe Condenser Model

A diagram of a typical heat-pipe condenser section is shown in Fig. 5, where the thicknesses of the pipe and liquid wick are b_p and

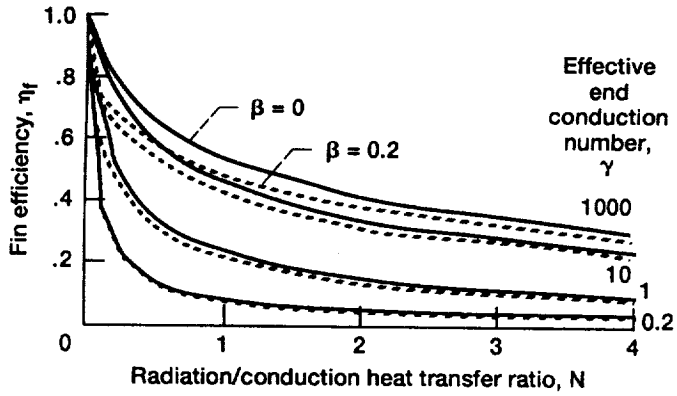

Figure 3.—Radiator fin efficiency function.

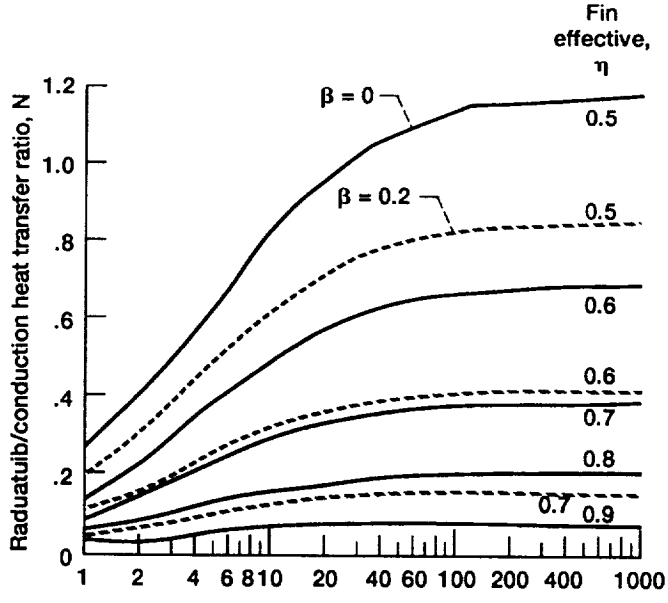

Figure 4.—Radiator fin design chart.

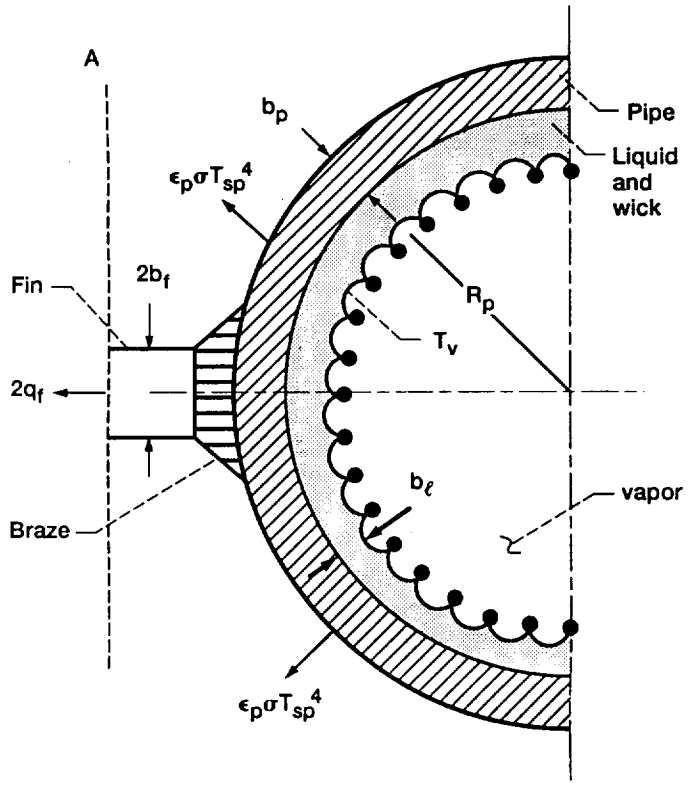

Figure 5.—Diagram of the fin/heat-pipe interface.

b_l, respectively, and where the pipe is connected to the fin through a brazing, for example, with contact conductance, h_c. Thus, the effective thermal resistance between the wick surface at vapor temperature ($T_e = T_v$) and the fin root can be written as

$$\frac{1}{h_e} = \frac{1}{S}\left(\frac{1}{h_c} + \frac{b_p}{k_p} + \frac{b_l}{k_l}\right) \tag{27}$$

where S is a shape factor introduced to account for circumferential conduction in the pipe and liquid materials. The precise determination of S requires a fully two-dimensional analysis of the composite region, which is beyond the scope of the present paper. It is noted, however, that the circumferentially constant temperature of the wick surface effectively limits the two-dimensional effect for heat flow into the fin, and we take S = 1.25 to 1.50. This contrasts with shape factors for convection pipes where the bulk fluid temperature is specified instead of a surface temperature (Lund, 1986, 1989).

Because of this condition, there will be considerable direct heat rejection from the surface of the pipe at temperature T_{sp}, effectively limiting the optimum fin length. The heat flux through the pipe wall is

$$q_p'' = \frac{T_v - T_{sp}}{\frac{b_p}{k_p} + \frac{b_l}{k_l}} = \epsilon_p \sigma T_{sp}^4 \tag{28}$$

Or, in terms of a pipe direct heat rejection efficiency

$$q_p'' = \eta_p \epsilon_p \sigma T_v^4 \tag{29}$$

where, from Eq. (28), the pipe efficiency is determined from

$$\eta_p - (1 - \delta\eta_p)^4 = 0 \tag{30}$$

and where the pipe radiation/resistance parameter is

$$\delta = \epsilon_p \sigma T_v^3 (b_p/k_p + b_l/k_l) \tag{31}$$

For the range, $0 < \delta < 1$, Eq. (30) is well represented by

$$\eta_p = 1 - 0.736\delta^{(0.252 - 0.0868 \ln\delta)} \tag{32}$$

With these definitions, the total heat transfer rate from one quarter of the pipe may be written as the sum

$$q_t = q_p + q_f = \sigma T_v^4 (\eta_p \epsilon_p P_p + \eta_f \epsilon L) \tag{33}$$

where the quarter-pipe effective perimeter is

$$P_p = \pi R_p/2 - b_f S \tag{34}$$

Equation (33) is the basis for the optimization calculations in the following section.

In this analysis the fin/pipe radiative interaction has been neglected for simplicity. This effect on overall heat rejection may be estimated from previous results (Sparrow and Cess, 1978), and a correction factor of 0.9 is used in Eq. (33); it is unlikely to have significant effect on the fin optimization.

OPTIMIZATION PROCEDURE

The optimization procedure used to determine the results given in this paper is presented here. The procedure was incorporated into a computer code, and several heat-pipe/fin combinations were analyzed.

Determination of Fin Thickness and Length

In order to determine the optimum fin geometry, the following in-puts are required: fin efficiency, surface Biot number, fin length, material thermal conductivities and densities, heat-pipe geometry and operating temperature. With this information, and specified S, Eq. (27) is used to calculate an effective thermal conductance h_e between the inner surface of the heat-pipe wick and the fin root. Next, the effective end-conduction number γ is calculated with Eq. (23). With γ, fin efficiency η_f, and an estimated surface Biot number β, the radiation conduction number N can be found from Fig. 4. Finally, the fin thickness b_f is calculated using Eq. (16). This procedure is repeated for several different fin lengths until an optimum length is found. With the fin geometry fixed, a surface Biot number β is calculated and compared with the initial estimate. If there is a significant difference between the two, the calculation is repeated with the new β. However, in the cases considered, β remained a very small number, on the order of 10^{-4}, and iterations were unnecessary.

Criterion Function

The objective of the optimization procedure is to minimize the overall mass per thermal power dissipated (C, kg/kW), for the heat pipe and fin configuration. This gives a fin-tube arrangement which gives the maximum heat transfer per overall mass. One quarter of the mass per unit length of a heat-pipe and half of the fin is

$$M = \rho_f b_f L + \rho_p A_p + \rho_l A_l \tag{35}$$

where ρ_f, ρ_p, and ρ_l are the densities of the fin material, pipe material and heat-pipe working fluid, respectively. A_p and A_l are one-fourth the cross-sectional area of both heat-pipe material and heat-pipe working fluid, respectively. Half the total fin thickness is b_f. The total heat transfer from the heat pipe and fin (q_t) is calculated using Eq. (33). The criterion function C, which represents the ratio of the mass of the heat-pipe and fin over the heat transfered, can then be calculated as

$$C = M/q_t \qquad (36)$$

The criterion function is calculated for a range of fin lengths and thicknesses generated from the calculation procedure discussed here. The fin length which yields the lowest C is chosen as optimum. Subsequently, conditions at this minimum, or optimum, are designated by a superscript asterisk; for example, the minimum value of the criterion is denoted C^*.

Minimum-Mass Condition

The procedure outlined in the preceding section to determine fin thickness and criterion function was incorporated into a computer code and used to model several different heat-pipe radiators. An aluminum heat pipe with aluminum fins and ammonia as a working fluid was modeled. Property data for this analysis are summarized in Table I. Results from the analysis are shown in Fig. 6. The manner in which the criterion function varies with fin length for several different fin efficiency values is shown. It is interesting that the highest fin efficiency, $\eta_f = 0.9$, does not always yield the lowest criterion function C. The minimum value of C was calculated to be 1.26 kg/kW. This value corresponds to a fin efficiency of 0.5 and a fin length of 8.5 cm, which compares well with previous results with specified root temperature (Sparrow and Cess, 1978; Bartas and Sellers, 1960). There are a range of fin lengths and fin efficiency values which yield C values very close to the minimum of 1.26. Several combinations of parameters between fin lengths of approximately 3 to 13 cm yield C values close to the minimum. This shows that in this particular case the radiator designer can use some discretion in choosing the optimum fin length, based on considerations other than thermal performance such as structural integrity, stowage volume, and survivability, etc.

TABLE I. - INPUT PARAMETERS FOR 400 K RADIATOR MODEL

	Fin material		
	Gr/Al	Be/Al	C-C/Al
Working fluid	NH_3	NH_3	NH_3
Biot number Thermal conductivity, W/mK	8.1×10^{-7}	3.4×10^{-7}	6.3×10^{-7}
Fin length	Varied	180	Varied
Fin transverse	77	180	10
Pipe wall	77	180	10
Wick	40	40	40
Contact thermal Conductance between pipe and fin, W/mK	1×10^9	1×10^9	1×10^9
Material density, g/cm^3			
Fin	2.702	1.850	1.69
Pipe	2.702	1.850	1.69
Wick material	2.702	1.850	2.80
Heat pipe fluid	0.37	0.37	0.37
Wick porosity	0.7	0.7	0.7
Heat pipe o.d. cm	1.5	1.5	1.5
Shape factor, pipe/fin	1.0	1.0	1.0
Pipe wall thickness, mm	1.0	1.0	1.0
Wick thickness, mm	1.0	1.0	1.0
Emissivity			
Fin	0.9	0.9	0.9
Pipe	0.9	0.9	0.9
Vapor temperature	400 K	400 K	400 K
Sink temperature	225 K	225 K	225 K
Radiation correction factor	0.9	0.9	0.9

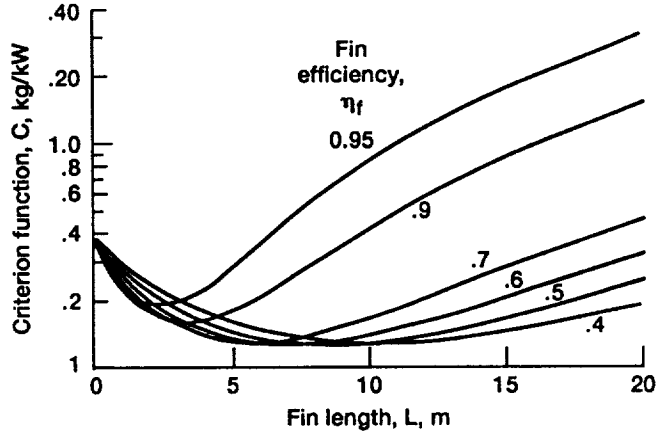

Figure 6.—Criterion function versus fin length for several fin efficiencies (β = 0; aluminum with ammonia heat-pipe fluid, geometry per table I).

RESULTS

Several heat-pipe and fin configurations made from different material combinations are modeled here. Metal matrix composites with graphite fibers, carbon-carbon, and beryllium are the fin and tube materials chosen for this analysis. The analysis is performed at two different vapor temperatures: 400 and 800 K. Two common heat-pipe working fluids are used; ammonia at 400 K and potassium at 800 K. Heat-pipe containment envelop materials are chosen which are compatible with the respective working fluid. The geometry of the heat-pipe is kept constant throughout the analysis. The results of this analysis yield an interesting comparison of some common space radiator materials.

Graphite/aluminum, carbon/carbon, and beryllium fin and tube configurations are designed here for operation at 400 K. Ammonia is used as the heat-pipe working fluid and aluminum as the wick and liner material for all three cases. Table I lists the input parameters for this analysis. The results of the analysis are shown in Fig. 7. Two fin efficiencies ratios are shown for each case, $\eta_f = 0.5$ and $\eta_f = 0.9$. These two values will typically bound the range of choices the radiator designer will have as shown in the optimization procedure section. Figure 7 shows a plot of the criterion function C^* versus axial thermal conductivity of the fin material. Axial thermal conductivity is varied because of the large variety of carbon

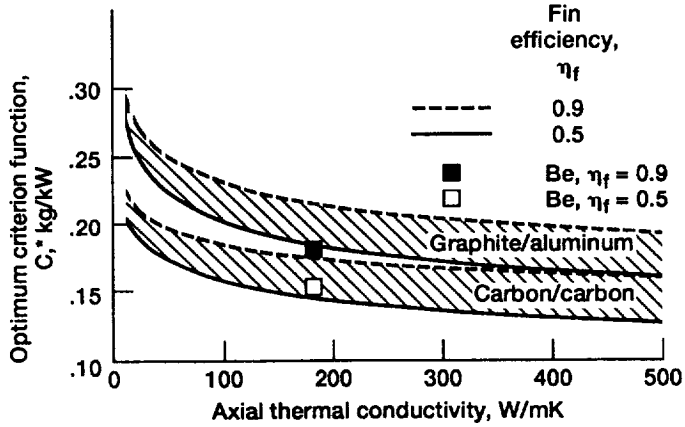

Figure 7.—Criterion function as a function of fin axial thermal conductivity for three materials at two fin efficiencies ratios operating at a temperature of 400 K.

fibers available for use in the carbon or metal matrix composites. The thermal conductivity of these fibers can vary from under 10 W/mK to over 500 W/mK. However, the axial thermal conductivity of beryllium is fixed. Therefore, the results for this case are represented by two points, as shown in Fig. 7.

The results show that for a given axial thermal conductivity, carbon/carbon is superior to both beryllium and graphite/aluminum. With P100 graphite fibers the axial thermal conductivity of graphite/aluminum and carbon/carbon is calculated to be 306 and 311 W/mK, respectively (Materials Science Corporation, 1986). Specific thermal conductivities (axial thermal conductivity over density) of graphite/aluminum with P-100 fibers, carbon/carbon with P-100 fibers, and beryllium are 121, 184, and 97 $(W/mK)/(g/cm^3)$, respectively. The specific thermal conductivity of graphite aluminum with P-100 fibers is significantly greater than beryllium, however the beryllium yields a radiator design with a lower criterion function. This shows that materials with the highest specific thermal conductivity are not always the best material for a radiator application. This contrasts with earlier assumptions (McDanels et al., 1991). Low density appears to be more important than high thermal conductivity for this design. Also, the transverse thermal conductivity of the composite does not appear to significantly affect the criterion function. The transverse thermal conductivity of the carbon/carbon is significantly lower than graphite/aluminum and beryllium as shown in Table I. However, with both a low density and high axial thermal conductivity, the carbon/carbon is still shown to be superior to the other materials.

A similar analysis was performed with graphite/copper, carbon/carbon, and beryllium operating at 800 K. Potassium is the heat-pipe working fluid, and the wick and liner material is titanium for all three cases. The input parameters for this analysis are listed in Table II. The results of this analysis are shown in Fig. 8. Again,

TABLE II. - INPUT PARAMETERS FOR 800 K RADIATOR MODEL

	Fin material		
	Gr/Cu	Be/Ti	C-C/Ti
Working fluid	K	K	K
Biot number	2.4×10^{-6}	4.8×10^{-6}	8.7×10^{-5}
Thermal conductivity, W/mK			
Fin length	Varied	109	Varied
Fin transverse	241	109	10
Pipe wall	241	109	10
Wick	7	7	7
Contact thermal Conductance between pipe and fin, W/mK	1×10^{9}	1×10^{9}	1×10^{9}
Material density, g/cm^2			
Fin	4.88	1.850	1.69
Pipe	4.88	1.850	1.69
Wick material	4.51	4.51	4.51
Heat pipe fluid	0.70	0.70	0.70
Wick porosity	0.7	0.7	0.7
Heat pipe o.d., cm	1.5	1.5	1.5
Shape factor, pipe/fin	1.0	1.0	1.0
Pipe wall thickness, mm	1.0	1.0	1.0
Wick thickness, mm	1.0	1.0	1.0
Emissivity			
Fin	0.9	0.9	0.9
Pipe	0.9	0.9	0.9
Vapor temperature	800 K	800 K	800 K
Sink temperature	225 K	225 K	225 K
Radiation correction factor	0.9	0.9	0.9

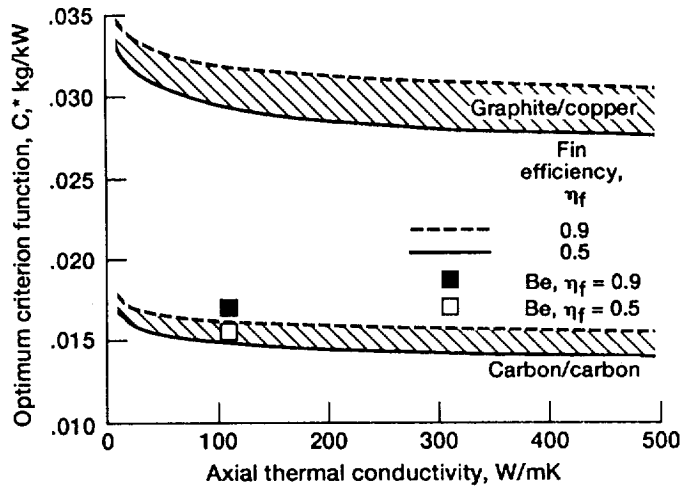

Figure 8.—Optimum criterion function versus fin axial thermal conductivity for three materials at two fin efficiencies operating at a temperature of 800 K.

the carbon/carbon design yields the lowest criterion function. The two beryllium cases are very close to the carbon/carbon case for the same axial thermal conductivity. The graphite/copper design yields a criterion function much higher than the beryllium case even though the specific thermal conductivity of graphite/copper is greater than beryllium: 96 and 59 $(W/mK)/(g/cm^3)$, respectively. This evidently results from the rather weak K_x dependence of C^*, and the density proportional behavior of C^* in Eqs. (34) and (35).

It has been shown that the fin transverse conduction effect is negligible, except near the fin/pipe interface where two-dimensional conduction plays a role. This is incorporated in the shape factor S, where a larger value of S represents a larger two-dimensional effect in the fin root and heat-pipe wall, and S = 1 represents one-dimensional radial conduction only.

The effect of S on C^* is shown with an analysis of heat pipes and fins made of beryllium with potassium as the heat-pipe working fluid. The heat-pipe vapor temperature is 800 K. Figure 9 shows C^* is reduced with an increase in the two-dimensional (or circumferential) conduction effect. This is expected as a greater "grouping" of energy at the root. Although beneficial, a shape factor in excess of 1.5 is not expected for heat-pipe geometries as in Fig. 5, without special provision; exact evaluation of S requires a detailed, two-dimensional analysis of the interface region. Also evident in Fig. 9 is the effect of fin efficiency on C^*, with 0.5 the value for minimum C^*.

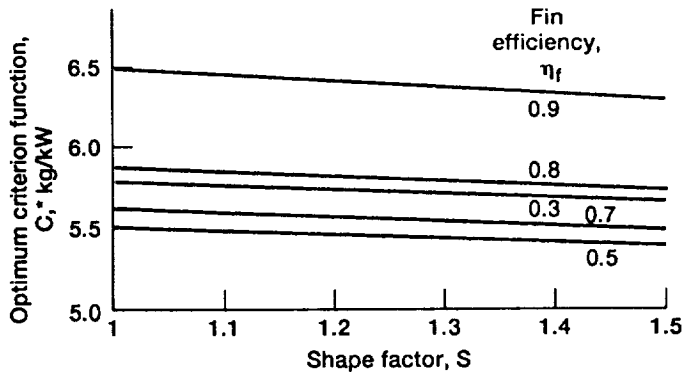

Figure 9.—Effect of shape factor on optimized performance index for beryllium/potassium heat-pipe/fin radiator panel.

CONCLUSION

The analysis presented here shows that using specific thermal conductivity is not a good figure of merit for radiator materials. The results of the analysis showed that the density of a radiator material is much more critical than the axial thermal conductivity of that material in order to obtain maximum heat transferred with minimum mass. Also, the transverse thermal conductivity of a composite fin material is shown to have only a minor effect on the criterion function for the radiator designs analyzed.

REFERENCES

Bartas, J.G., and Sellers, W.H., 1960, "Radiation Fin Effectiveness," *Journal of Heat Transfer*, Vol. 82, pp. 73-75.

Edwards, D.K., 1981, *Radiation Heat Transfer Notes*, Hemisphere Publishing, Washington, D.C.

Furukawa, M., 1981, "Design and Off-Design Performance Calculations of Space Radiators," *Journal of Spacecraft and Rockets*, Vol. 18, No. 6, pp. 515-526.

Kakac, S., and Yener, Y., 1985, *Heat Conduction*, 2nd Ed., Hemisphere Publishing, Washington, D.C.

Lund, K.O., 1986, "General Thermal Analysis of Parallel-Flow Flat-Plate Solar Collector Absorbers," *Solar Energy*, Vol. 36, pp. 443-450.

Lund, K.O., 1989, "General Thermal Analysis of Serpentine-Flow Flat-Plate Solar Collector Absorbers," Journal of Solar Energy, Vol. 42, pp. 133-142.

Lund, K.O., 1990, "Application of Finite-Time Thermodynamics to Solar Power Conversion," *Finite-Time Thermodynamics and Thermoeconomics*, (Advances in Thermodynamics, Vol. 4), S. Sieniutycz and P. Salamon, Eds., Taylor & Francis, New York, pp. 120-138.

Materials Sciences Corporation, 1986, "Satellite Applications for Carbon-Carbon: Brazed and Mechanical Joint Design," Technical Final Report MSC-TFR-1708/2001.

McDanels, D.L., Baker, K.W. and Ellis, D.L., 1991, "Graphite Fiber/Copper Matrix Composites for Space Power Heat Pipe Fin Applications," *Eighth Symposium on Space Nuclear Power Systems*, CONF-910116, DOE, ppl. 313-319.

Rhee, H.S., Begg, L., Wetch, J.R., and Juhasz, A.J., 1991, "Advanced Radiator Concepts Feasibility Demonstration," *Eighth Symposium on Space Nuclear Power Systems*, CONF-910116, DOE, pp. 708-713.

Rovang, R.D., Hunt, M.E., Dirling, R.B., and Holzl, R.A., 1991, "SP-100 High-Temperature Advanced Radiator Development," *Eighth Symposium on Space Nuclear Power Systems*, CONF-910116, DOE, pp. 702-707.

Siegel, R., and Howell, J.R., 1981, *Thermal Radiation Heat Transfer*, 2nd Ed., Hemisphere Publishing, Washington, D.C.

Sparrow, E.M., and Cess, R.D., 1978, *Radiation Heat Transfer*, Augmented Edition, Hemisphere Publishing, Washington, D.C.

REPORT DOCUMENTATION PAGE

Form Approved
OMB No. 0704-0188

1. AGENCY USE ONLY (*Leave blank*)	2. REPORT DATE	3. REPORT TYPE AND DATES COVERED
	1991	Technical Memorandum

4. TITLE AND SUBTITLE

Effects of Anisotropic Conduction and Heat Pipe Interaction on Minimum Mass Space Radiators

5. FUNDING NUMBERS

WU-590-13-21

6. AUTHOR(S)

Karl W. Baker and Kurt O. Lund

7. PERFORMING ORGANIZATION NAME(S) AND ADDRESS(ES)

National Aeronautics and Space Administration
Lewis Research Center
Cleveland, Ohio 44135-3191

8. PERFORMING ORGANIZATION REPORT NUMBER

E-6636

9. SPONSORING/MONITORING AGENCY NAMES(S) AND ADDRESS(ES)

National Aeronautics and Space Administration
Washington, D.C. 20546-0001

10. SPONSORING/MONITORING AGENCY REPORT NUMBER

NASA TM-105297

11. SUPPLEMENTARY NOTES

Prepared for the International Solar Energy Conference sponsored by the American Society of Mechanical Engineers, Maui, Hawaii, April 4-8, 1992. Karl W. Baker, NASA Lewis Research Center; Kurt O. Lund, University of California, San Diego, San Diego, California 92037. Responsible person, Karl W. Baker, (216) 433-6162.

12a. DISTRIBUTION/AVAILABILITY STATEMENT

Unclassified - Unlimited
Subject Category 20

12b. DISTRIBUTION CODE

13. ABSTRACT (*Maximum 200 words*)

Equations are formulated for the two-dimensional, anisotropic conduction of heat in space radiator fins. The transverse temperature field is obtained by the integral method, and the axial field by numerical integration. A shape factor, defined for the axial boundary condition, simplifies the analysis and renders the results applicable to general heat-pipe/conduction-fin interface designs. The thermal results are summarized in terms of the fin efficiency, a radiation/axial-conductance number, and a transverse-conductance surface Biot number. These relations, together with those for mass distribution between fins and heat pipes, are used in predicting the minimum radiator mass for fixed thermal properties and fin efficiency. This mass is found to decrease monotonically with increasing fin conductivity. Sensitivities of the minimum-mass designs to the problem parameters are determined. Further, detailed investigation of the fin/heat-pipe interaction is recommended for future work.

14. SUBJECT TERMS

Radiator; Heat pipes; Fins; Code

15. NUMBER OF PAGES

10

16. PRICE CODE

17. SECURITY CLASSIFICATION OF REPORT	18. SECURITY CLASSIFICATION OF THIS PAGE	19. SECURITY CLASSIFICATION OF ABSTRACT	20. LIMITATION OF ABSTRACT
Unclassified	Unclassified	Unclassified	